FORMULATION AND COMPARISON OF SPRAY DRIED NON-POROUS AND LARGE POROUS PARTICLES CONTAINING MELOXICAM FOR PULMONARY DRUG DELIVERY

ANITA CHVATAL[1], RITA AMBRUS[1], PETRA PARTY[1], GÁBOR KATONA[1], ORSOLYA JÓJÁRT-LACZKOVICH[1], PIROSKA SZABÓ-RÉVÉSZ[1], ELIAS FATTAL[2], NICOLAS TSAPIS[2*]

[1] University of Szeged, Faculty of Pharmacy, Institute of Pharmaceutical Technology and Regulatory Affairs, Szeged, Hungary
[2] Institut Galien Paris-Sud, CNRS, Univ. Paris-Sud, Université Paris-Saclay, 92296 Châtenay-Malabry, France.

*Co-corresponding authors:
Nicolas Tsapis
Institut Galien Paris-Sud, CNRS, Univ. Paris-Sud, Université Paris-Saclay, 92296 Châtenay-Malabry, France.
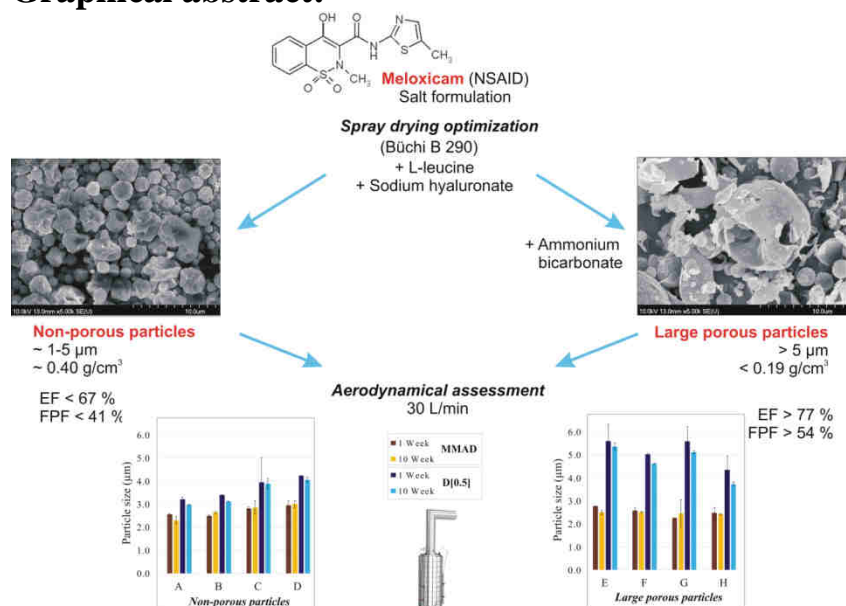
and

Rita Ambrus
University of Szeged, Faculty of Pharmacy, Institute of Pharmaceutical Technology and Regulatory Affairs, Szeged, Hungary

Graphical abstract:

Abstract:

Meloxicam is an anti-inflammatory drug that could be interesting to deliver locally to the lungs to treat inflammation occurring in cystic fibrosis or chronic obstructive pulmonary disease (COPD). Spray drying conditions were optimized to prepare inhalable dry powders, from meloxicam aqueous solution with pH adjustment. A comparison study between non-porous and large porous particles (LPPs) was carried out to demonstrate the relevance of the aimed large size (>5 µm) and low density (<0.2 mg/cm^3) formulations. With the appropriate amount of porogen agent, ammonium bicarbonate, LPPs exhibited the same aerodynamic diameter and a higher deposited fraction than smaller but dense particles. The aerodynamic evaluation of LPPs showed that the fine particle fraction (FPF) reached up to 65.8%, while the emitted fraction (EF) reached 85.4%, both higher than for the non-porous particles. Stability tests demonstrated that, after 10 weeks of storage, no significant difference could be detected in the aerodynamic behaviour of the formulations. To the best of our knowledge this is the first time large porous particles, with enhanced aerodynamic properties, from an aqueous solution of meloxicam are reported.

Footnote
AB – Ammonium Bicarbonate
API – Active Pharmaceutical Ingredient
CF – Cystic Fibrosis
COPD – Chronic Obstructive Pulmonary Disease
D[0.5] – Median Geometric Diameter
DPI – Dry Powder Inhaler
EF – Emitted Fraction
FPF – Fine Particle Fraction
HA – Sodium Hyaluronate
LEU – L-Leucine
LPPs – Large Porous Particles

MMAD – Mass Median Aerodynamic Diameter
MX – Meloxicam
NSAID – Non Steroidal Anti-Inflammatory Drug
SD – Spray Dried

1   Introduction

In the past decades, carrier-free dry powder inhalers (DPIs) have shown promises for the local pulmonary treatment of chronic obstructive pulmonary disease (COPD) and cystic fibrosis (CF). In carrier-free formulations, active pharmaceutical ingredients (APIs) and excipients are formulated together into the inhalable DPI form without using large carriers such as lactose *(Hoppentocht et al., 2014)*.

For pulmonary disorders with increased inflammation, the use of non-steroidal anti-inflammatory drugs (NSAIDs), such as ibuprofen, diclofenac, gained the attention of research studies *(Szabó-Révész, 2018)*. Among NSAIDs, meloxicam (MX) is a low water-soluble cyclooxygenase enzyme-2 selective inhibitor, which has anti-inflammatory and antioxidant effects. Due to these effects, MX could be of interest for pulmonary administration to locally treat CF, COPD or any other lung inflammation *(Tsubouchi et al., 2000; Arafa et al., 2007)*.

So far, literature data reported preparation of MX containing inhalable microparticles by pre-suspension spray drying method. Pomázi et al. described the preparation MX particles suspended in an aqueous solution of excipients (mannitol, poly-vinyl-alcohol, polyvinylpyrrolidone and leucine) which was then spray dried at 130 °C to produce inhalable microparticles with enhanced aerodynamic properties *(Pomázi et. al., 2011; Pomázi et al, 2013; Pomázi et al, 2014)*. Due to the preparation method, MX was in crystalline form in the formulations. Another option for the inhalable microcomposite preparation is the use of MX potassium salt form and additional excipients (Poly-vinyl alcohol, leucine) *(Chvatal et al, 2017)*. Due to the water solubility of the MX salt *(Mezei et al., 2009)*, an easier feed stock preparation and spray drying conditions could be developed, leading to amorphous MX *(Chvatal et al., 2017)*.

The newest DPI researches report about several high potency carrier-free formulations prepared by spray drying. Co-spray drying has been widely used in the DPI production because it is scalable and offers an easily controlled particle formulation. Besides using this process for the micronization of the API, it can also lead to good aerodynamic properties for products *(Healy et al., 2014)*. Innovative formulations by spray drying can be produced to create special structure (e.g. porous particles) and appropriate morphology of the API both for carrier-based and for carrier-free formulations *(Tsapis, 2014)*.

Carrier-free formulation aimed to reduce the intrinsic cohesion of the particles, increase dispersion and delivery from the inhaler. Special excipients are used (for e.g. amino acids, polymers, bulking agents, phospholipids) in the particle design phase to implement also low density and enhanced aerosolization of the particles *(Healy et al., 2014)*.

Among widely used excipients to increase the aerosolization behaviour of the particles are leucine (LEU) and its analogues such as tri-Leucine *(Lechuga-Ballesteros et al, 2008; Vehring, 2008)*. LEU was shown to promote good aerosolization of the particles by decreasing the surface energy (cohesive and adhesive forces) between particles as it is accumulates at particle surface *(Raula et al., 2010)*. It was also demonstrated that the LEU (above 20%, w/w content) may recrystallizes during the spray drying covering the surface of the particle and protecting it against moisture *(Li et al., 2016)*.

Biodegradable polymers, such as sodium hyaluronate (HA), are also used to enhance the aerosolization of the API. HA can be used in the pulmonary drug delivery as a drug targeting, due to its mucoadhesive characteristics, absorption promoter and structure stabilizing effect *(Martinelli et al., 2017)*. HA also increases the viscosity of the primary solution to obtain large droplets for spray drying and thus larger particle sizes.

The aerodynamic performance of the DPIs also depends on the density of the powder. Particles with low density have better flowability and can be delivered to the lung easier with higher deposition *(Bosquillon et al., 2001)*. An exact density value is not clearly established, but most of the studies consider the DPI "low density" from a tap density around 0.4-0.1 g/cm^3 or lower *(Ogienko et al., 2017; Ógáin et al., 2011; Watts et al., 2013)*. Large porous particles (LPPs) can be obtained using porogen agents (e.g. volatile liquids, ammonium carbonate or bicarbonate) in the primary solutions or emulsions (*Gervelas et al., 2007*). The porogen evaporates quicker than the dispersion phase is drying, leaving holes in the interior of the larger sized particles (*N'Guessan et al., 2018; Pham et al., 2013*). The formulation of stable structured LPPs with the appropriate excipient-API concentration and production properties may be the challenge of the pharmaceutical technology.

We aimed to produce LPPs from MX aqueous solution by forming an MX salt at high pH. For this, we have optimized the spray drying procedure, by varying the solution excipient concentration. The planned LPPs with particle size larger than 5 µm and tap density lower than 0.25 g/cm^3 should be endowed with enhanced aerosolization properties (*Cruz et al., 2011*). The efficacies of the prepared LPPs were compared with non-porous formulations by their spray drying yield, physical chemical properties, morphology and *in vitro* aerodynamic behaviour. To the best of our knowledge, no other studies on the formulation of inhalable LPPs containing MX from solution exist.

2 Materials and methods

2.1 Materials
Meloxicam (MX) was obtained from Egis Plc (Hungary). L-Leucine (LEU) and ammonium bicarbonate (AB) were purchased from Sigma-Aldrich (France) and sodium hyaluronate (HA) from Acros Organics (Belgium). Sodium hydroxide was obtained from Sigma-Aldrich (France). Water was purified using a RIOS/MilliQ system from Millipore (France).

2.2 Preparation of the spray dried microparticles
MX exhibits a pH dependent solubility: in buffers at pH 7.4-7.7 MX demonstrates almost 43 fold solubility (1.74±0.2 mg/mL, 37 °C) at this pH than in distilled water (0.04±0.01 mg/mL, 37 °C) (*Horváth et al, 2016*). Due to this characteristic, MX was dissolved at room temperature (18-20 °C) at higher pH, stabilized with 1 M sodium hydroxide aqueous solution, to prepare a stock solution for the spray drying. First, MX was dissolved in the high pH water (8.00±0.1 pH, stirring for 2 hours, 600 rpm) at a constant concentration of 1.5 mg/mL for each formulation. Secondly, in the MX solution, LEU was dissolved (15 min, 600 rpm) to reach a final concentration of 0.75 mg/mL. In some cases, HA was added to finally yield a HA concentration

of 0.15, 0.30 or 0.45 mg/mL (HA solutions were prepared the day before spray drying, stirring for 24 hours, 400 rpm). These solutions containing MX, MX+LEU or MX+LEU+HA were used for the formulation of non-porous particles. For LPP formulations, different concentrations of AB were added (0.5, 1.5 and 2.0 mg/mL) which functions as porogen agent as it decomposes into CO_2 and H_2O upon heating. AB was dissolved 5 min before the spray drying (stirring for 2 min, 200 rpm) to minimize its decomposition prior to spray drying. The inhalable microparticles were produced by spray drying using a Büchi B-290 spray dryer equipped with a 0.7 mm two-fluid nozzle (Büchi, Switzerland). Drying properties were the followings: 200 °C inlet temperature, 9 mL/min feed pump rate (30%), 100% aspirator rate, and 414 L/h gas flow rate.

The spray drying yield was calculated as a percentage by dividing the mass of the powder collected from the container by the initial mass of solids in the solution prepared for drying. Prepared powders were stored in desiccator containing cobalt crystals to decrease moisture uptake (at 23±1 °C).

2.3 Identification of spray dried API

To investigate the characteristics of the API in the formulations, Raman spectroscopy was applied using Thermo Fisher DXR Dispersive Raman with CCD camera (Thermo Fisher Sco. Inc., Waltham, MA, USA). Following parameters were used during measurements: laser diode operating at a wavelength of 780 nm; the applied laser power was 6-24 mW at 25 µm slit aperture size on a 2 µm spot size; spectra were collected with 6 sec exposure time of 20 scanning in the spectral range of 3300-200 cm^{-1}. Reference sample, MX-recrystallized, was obtained with dissolving MX with the same method as MX solutions were prepared for spray drying. 1.5 mg/mL MX was dissolved in 8±0.1 pH sodium hydroxide aqueous solution (stirring for 2 hours, 600 rpm) and dried out at 40 °C, for 24 hours to study the changes during dissolution.

The actual API content (%) after spray drying was measured by dissolving 1.0-1.1 mg formulation in 25 ml of methanol:pH 7.4 phosphate buffer (60:40%, v/v), which solution was used for the aerodynamic assessment also. Solutions were mixed for 10 min, 600 rpm and API content was quantified by UV/Vis spectrophotometry (ATI-UNICAM UV/VIS Spectrophotometer, Cambridge, UK) at 362 nm wavelength. Each sample was measured in triplicate. The calibration curve y= 0.00465x, R^2=0.9994 was used for quantification. Values LOD (0.037 µg/mL) and LOQ (0.124 µg/mL) were also established.

2.4 Morphology

Scanning electron microscopy (SEM) (Hitachi S4700, Hitachi Scientific Ltd., Tokyo, Japan) was used to characterize the morphology of the spray dried formulations, applying 10 kV high voltage and 1.3-13.0 mPa air pressure. A high vacuum evaporator and argon atmosphere was used to sputter-coat samples with gold-palladium in order to make them conductive (Bio-Rad SC 502, VG Microtech, Uckfield, UK).

2.5 Particle size distribution

The geometric diameter of the particles was established using laser diffraction (Mastersizer 2000 equipped with a Sirocco dry disperser, Malvern Instruments, France). For the measurements a micro size plate was used at a dispersing pressure of 2 bars. Each sample was measured in triplicate. The particle size distribution was characterized by the D[0.1] (10% of the volume distribution is below this value), D[0.5] (the volume median diameter is the diameter where 50% of the distribution is above and 50% is below) and D[0.9] (90% of the volume distribution is below this value) values. The size distribution Span was calculated according to **Eq. 1**. A high Span value denotes a broad particle size distribution. The higher the Span value, the broader the particle size distribution is (*Li et al., 2004*). All samples were measured in triplicate.

$$\text{Span} = \frac{D[0.9] - D[0.1]}{D[0.5]}$$ (**Eq. 1**)

2.6 Density measurements

The density of the formulations was measured using a 5 mL cylinder, filled with 2-4 mL powder (for bulk density) and tapped 1000 times (for tap density) using a tapping apparatus (Pharma test PT-TD1) *(European Pharmacopeia 9th edition)*. All samples were measured in triplicate.

2.7 Structural analyses

To establish the crystalline or amorphous character of the spray dried samples, X-ray powder diffraction (XRPD) spectra were recorded with a BRUKER D8 Advance X-ray diffractometer (Bruker AXS GmbH, Karlsruhe, Germany) system with Cu Kα1 radiation (λ = 1.5406 Å) over the interval 3-40°. Measurement conditions were as follows: target, Cu; filter, Ni; voltage, 40 kV; current, 40 mA; time constant, 0.1 s; angular step 0.010°.

2.8 Aerodynamic assessment

The aerosolization efficacy of the spray dried formulations was assessed *in vitro*, using an Andersen cascade impactor - Apparatus D, (*European Pharmacopeia 9th edition*), Copley Scientific, Switzerland). The inhalation flow rate was set at 30±1 L/min (High-capacity Pump Model HCP5, Critical Flow Controller Model TPK, Copley Scientific Ltd., Nottingham, UK). The inhalation time was 4 s for one inhalation simulation. Breezhaler® single dose devices were used, with size 3 capsules (transparent, Capsugel) filled with 2-2.5 mg of powder (constantly for each formulation). The inhaler was actuated twice for each capsule. The plates of the impactor were coated with 1 % w/v mixture of Span 85 and cyclohexane, to allow for the attachment of floating particles. After actuation, the inhalation device, the capsules, the induction port, the collection plates and the filter were washed with methanol:pH 7.4 phosphate buffer (60:40 %, v/v) to collect and dissolve the deposited API. The collected MX was quantified by UV/Vis spectrophotometry (ATI-UNICAM UV/VIS Spectrophotometer, Cambridge, UK) at 362 nm wavelengths.

Aerodynamic properties (Fine particle fraction – FPF and Mass median aerodynamic diameter – MMAD) were calculated from a plot of the cumulative percentage undersize of API on log probability scale against the effective cut-off aerodynamic diameter (*Colombo et al., 2012*). The emitted fraction (EF) was expressed as the percentage of the API found in the cascade impactor (except the API found in the capsules and device) after inhalation relative to the total loaded dose.

All the samples were measured at the 1st week after the spray drying and after 10 weeks of storage. Samples were stored at room temperature (23±1 °C), in a separate desiccator containing cobalt crystals to assess for their stability. Each sample was measured in triplicate. Statistical analyses were taken for the stability assessment using t-test calculation, 0.05 significance level and one-tailed hypothesis.

3   Results and discussion

Formulations were prepared according to Table I, by fixing MX concentration and varying the content in LEU and HA. In addition, non-porous particles (no AB added) were compared to LPPs prepared with AB.

Table I. Composition of the solutions prepared for spray drying (mg/mL) and the compositions of the spray dried products (%). MX=meloxicam, LEU=leucine, HA=sodium hyaluronate and AB=ammonium bicarbonate.

Sample names	MX	LEU	HA	AB*
Non-porous particles				
MX-SD	1.5 mg/mL (100%)	-	-	-
MX/LEU	1.5 mg/mL (66.7%)	0.75 mg/mL (33.3%)	-	-
MX/LEU/HA$^{0.3}$	1.5 mg/mL (58.8%)	0.75 mg/mL (29.4%)	0.30 mg/mL (11.8%)	-
MX/LEU/HA$^{0.15}$	1.5 mg/mL (62.5%)	0.75 mg/mL (31.2%)	0.15 mg/mL (6.3%)	-
Large porous particles				
MX/LEU/HA$^{0.3}$/AB$^{1.5}$	1.5 mg/mL (58.8%)	0.75 mg/mL (29.4%)	0.30 mg/mL (11.8%)	1.5
MX/LEU/HA$^{0.15}$/AB$^{1.5}$	1.5 mg/mL (62.5%)	0.75 mg/mL (31.2%)	0.15 mg/mL (6.3%)	1.5
MX/LEU/HA$^{0.3}$/AB^{2}	1.5 mg/mL (58.8%)	0.75 mg/mL (29.4%)	0.30 mg/mL (11.8%)	2.0
MX/LEU/HA$^{0.15}$/AB^{2}	1.5 mg/mL (62.5%)	0.75 mg/mL (31.2%)	0.15 mg/mL (6.3%)	2.0

*AB is not present in the dried samples as it decomposes into CO_2 and H_2O during spray drying.

3.1 Identification of API and drug content in the spray dried formulations
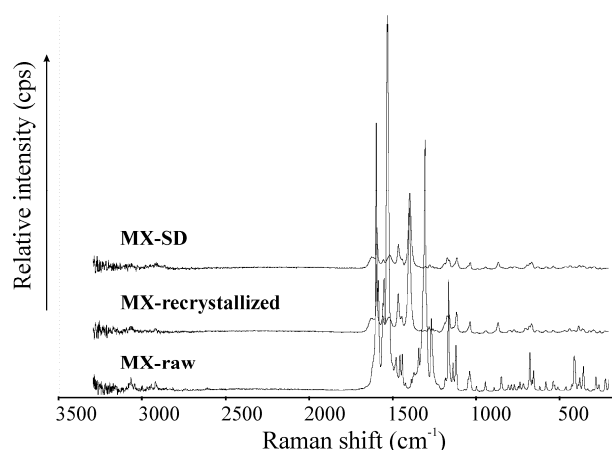

Fig. 1. Raman spectra of the raw MX (MX-raw), MX dissolved in sodium hydroxide at 1.5 mg/mL and dried out at 40 °C, 24 hours (MX-recrystallized) and spray dried MX (MX-SD).

The Raman spectrum of MX-raw exhibits characteristic bands at 1155, 1309, 1540 and 1595 cm^{-1} (**Fig. 1.**). MX-recrystallized shows difference at the 1390 cm^{-1} compared to MX-raw where this band is missing. However, there is no difference in the spectra of the spray dried and the recrystallized samples. These Raman spectra are similar to the spectra of MX sodium salt according to Bio-Rad Laboratories database (Bio-Rad Laboratories, Inc. SpectraBase; Meloxicam sodium). Based on this result it was established that during dissolution of MX (at pH 8±0.1 in sodium hydroxide aqueous solution) MX sodium salt form was obtained.
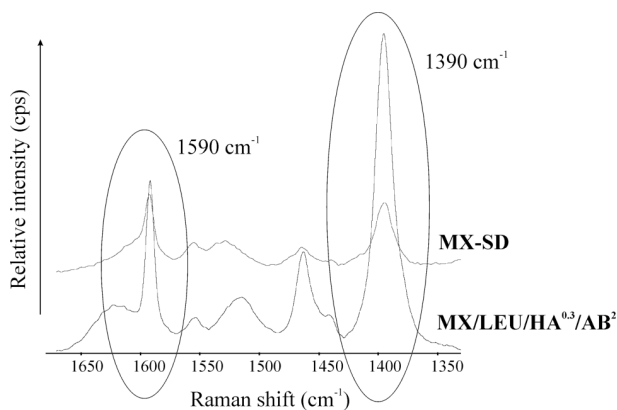

Fig. 2. Comparison of the Raman spectra of the spray dried MX (MX-SD) and one of the LPP formulations (MX/LEU/HA$^{0.3}$/AB^2).

Spray dried MX (MX-SD) and formulations with excipients (**Fig. 2**. MX/LEU/HA$^{0.3}$/AB^2 LPP formulation presented) exhibit the same spectra as MX sodium salt with characteristic Raman bands at 1390 and 1595 cm^{-1}, indicating MX sodium salt form is present in spray dried formulations.
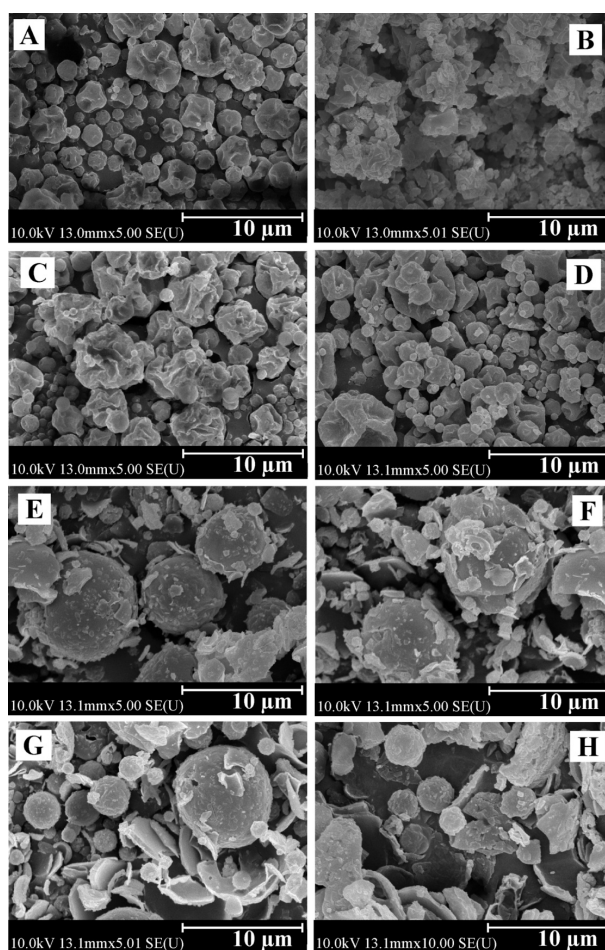
3.2 Particle morphology

Fig. 3. Scanning Electron Microscopy pictures of the non-porous particles (**A**: MX-SD, **B**: MX/LEU, **C**: MX/LEU/HA$^{0.3}$, **D**: MX/LEU/HA$^{0.15}$) and large porous particles (**E**: MX/LEU/HA$^{0.15}$/AB$^{1.5}$, **F**: MX/LEU/HA$^{0.15}$/AB^2, **G**: MX/LEU/HA$^{0.3}$/AB$^{1.5}$, **H**: MX/LEU/HA$^{0.3}$/AB^2).

From the SEM pictures, one can observe that the excipient free sample (A: MX-SD) exhibits a slightly rough surface and spherical-like shape (**Fig. 3.**). The same surface morphology was obtained with the spray drying of meloxicam potassium salt from aqueous solution (*Chvatal et al., 2017*). In other studies, the spray drying of meloxicam from aqueous suspension resulted in smooth surface particles with around 19 µm size (*Pomázi et al, 2011*). The presence of LEU increased the roughness of the surface and resulted in irregular-shaped particles (B: MX/LEU, C: MX/LEU/HA$^{0.3}$, D: MX/LEU/HA$^{0.15}$). The shape modification can be explained by the crystallization of LEU on droplet surface forming an external shell which collapses during the spray drying process *(Vehring, 2008)*. The surface accumulation of LEU and the resulting rough surface may reduce the adhesion between particles and the attachment to capsule or inhalation device walls, leading to higher EF or FPF values (*Aquino et al, 2012*; *Mangal et al., 2015*). With 0.15-0.30 mg/mL HA content (C: MX/LEU/HA$^{0.15}$ and D: MX/LEU/HA$^{0.3}$) the particles kept similar wrinkled surfaces and the polymer has no visible impact on the morphology. However, literature data report that sodium hyaluronate could promote surface roughness of spray dried salbutamol sulphate particles (*Li et al., 2017*). LPPs exhibit significantly different

morphology than non-porous formulations proving the essential role of the porogen agent AB. The SEM pictures further demonstrated the porogen effect of AB, which was an essential excipient for LPP formulation. Samples MX/LEU/HA$^{0.15}$/AB$^{1.5}$ (E), MX/LEU/HA$^{0.15}$/AB^{2} (F), MX/LEU/HA$^{0.3}$/AB$^{1.5}$ (G) and MX/LEU/HA$^{0.3}$/AB^{2} (H) present spherical shaped large sized particles. However the surface roughness of LPPs was much lower, slight wrinkles can be detected on the surface of the spherical particles. This change in shape could arise from the gas formation from AB during the drying procedure, which blows up the wrinkled structure (Fig. 3). This effect of AB is a well described in literature (*Cruz et al., 2011; Nolan et al., 2009; Gervelas et al., 2007*). Some of the broken shells demonstrate the internal hollow structure which reflects the porosity and low density.

3.3   Size distribution

Despite all the powders were prepared using similar drying parameters, the final particle size distributions were different (**Table II.**). The geometric diameter of spray dried MX was around 3 µm, nearly the same as the sample prepared with LEU (MX-SD 3.2 µm and MX/LEU 3.4 µm). Incorporating 0.75 mg/mL LEU in the formulation did not increase the geometric size of the MX containing particles as reported with other MX formulations using 0.6 g/L or higher LEU concentrations (*Pham et al, 2013*; *Chvatal et al, 2017*). Studies with different active ingredients also showed no effect of leucine concentration on particle size up to 20% w/w (*Aquino et al, 2012*) or only a low effect up to 15% w/w (*Mangal et al, 2015*). We demonstrated that the particle size is slightly increasing with an increasing amount of HA: from 3.4 µm up to 4.3 µm with 0.30 mg/mL HA. In case of LPPs the geometric size was also increased significantly with the higher HA concentration (from 5.0 µm to 5.6 µm with 0.15 and 0.30 mg/mL HA concentrations respectively). This increase probably arises from an increase of the viscosity of the spray dried solution leading to larger droplets and thus resulting in larger particle size. Li et al. also demonstrated that increased sodium hyaluronate concentration increases the particle size of co-spray dried salbutamol sulphate formulations from 3.8 µm up to 4.8 µm (0.20 and 0.35% w/w HA concentrations respectively) (*Li et al, 2017*). With addition of AB to the LEU and HA combination, we obtained the aimed larger geometric diameter (larger than 4.9 µm) due to the formation of pores (blowing effect) of AB, as AB decomposes into water and gas during the drying process (*Cruz et al., 2011; Pham et al, 2015*). No evident effect on the geometric size was detected comparing 1.5 and 2.0 mg/mL AB concentrations. Both non-porous particles and LPPs have narrow size distribution with Span ≤2.0. No significant differences were detected between the geometric diameter of the particles measured at 1st week and 10 weeks after of storage.

3.4   Density of the spray dried microparticles

As expected, non-porous particles have higher density than LPPs. Comparing the tap and bulk density, it can be established, that the difference between tap and bulk density of LPPs is lower than the difference between the same parameters for non-porous particles. This lower tap-bulk density differences indicates the better rearrangement of LPPs upon tapping. Briefly, from the density of the spray dried MX (MX-SD) and the formulation with 0.75 mg/mL of LEU (MX/LEU) it is clear that the presence of LEU increased the tap density from 0.36 up to 0.45

g/cm^3 (**Table II.**). However, the bulk densities of these two formulations were similar (0.23 and 0.27 g/cm^3). This can be explained with the rough surface LEU-containing particles: particles with rough surface or wrinkled shape can pack more efficiently and result in higher tap density *(Simon et al., 2016)*. Our results were similar with previous observations where leucine inclusion up to 15% (w/w) led to higher bulk density powders while up to 20% (w/w) produced powders with similar or slightly lower bulk density (*Aquino et al, 2012*). Results show that the HA content has no relevant influence on the density of the powders. Despite the fact that HA is increasing the viscosity of solutions, it has no significant effect on the density of dried particles. Without AB all the samples containing HA (MX/LEU/HA$^{0.15}$ and MX/LEU/HA$^{0.3}$) had a tap density around 0.42-0.47 g/cm^3. Low density of LPPs is related to the AB content which leads to the formation of a porous structure as it decomposes upon drying. The 2.0 and 1.5 mg/mL AB content have almost the same density decreasing effect and all the following samples (MX/LEU/HA$^{0.15}$/AB$^{1.5}$, MX/LEU/HA$^{0.15}$/AB^2, MX/LEU/HA$^{0.3}$/AB$^{1.5}$ and MX/LEU/HA$^{0.15}$/AB^2) reach tap density <0.19 g/cm^3.

Table II. Compositions of the non-porous and large porous particles, prepared with the optimized spray drying conditions (200 °C inlet temperature, 100% aspirator capacity, 9 mL/min feed pump rate, and 414 L/h gas flow rate), the spray drying characteristics (API content and spray drying yield), size distribution (D[0.5] = Median geometric diameter and Span) and density properties (bulk and tap density). Data are represented as mean ±S.D., n=3.

| Sample names	Spray drying yield (%)	Final API content (%)	D[0.5] (µm)	Span	Bulk density (g/cm^3)	Tap density (g/cm^3)
Non-porous particles						
MX-SD	88±2.76	89.7±1.3	3.2±0.08	1.4±0.08	0.23±0.02	0.36±0.06
MX/LEU	84±2.25	67.1±1.1	3.4±0.02	1.5±0.01	0.27±0.01	0.45±0.05
MX/LEU/HA$^{0.3}$	59±5.49	57.2±0.2	4.3±0.01	1.7±0.11	0.28±0.01	0.47±0.03
MX/LEU/HA$^{0.15}$	64±6.62	62.0±0.3	3.9±1.07	1.7±0.03	0.27±0.01	0.42±0.10
Large porous particles						
MX/LEU/HA$^{0.3}$/AB$^{1.5}$	62±2.13	53.6±2.1	5.6±0.73	2.0±0.10	0.09±0.01	0.14±0.01
MX/LEU/HA$^{0.15}$/AB$^{1.5}$	67±2.39	55.3±0.3	5.0±0.60	1.9±0.22	0.09±0.01	0.15±0.01
MX/LEU/HA$^{0.3}$/AB^{2}	62±2.07	50.7±1.0	5.6±0.64	2.0±0.13	0.07±0.02	0.10±0.02
MX/LEU/HA$^{0.15}$/AB^{2}	68±3.75	58.7±1.6	4.9±0.60	1.9±0.31	0.10±0.02	0.19±0.05

3.5 Structural analyses
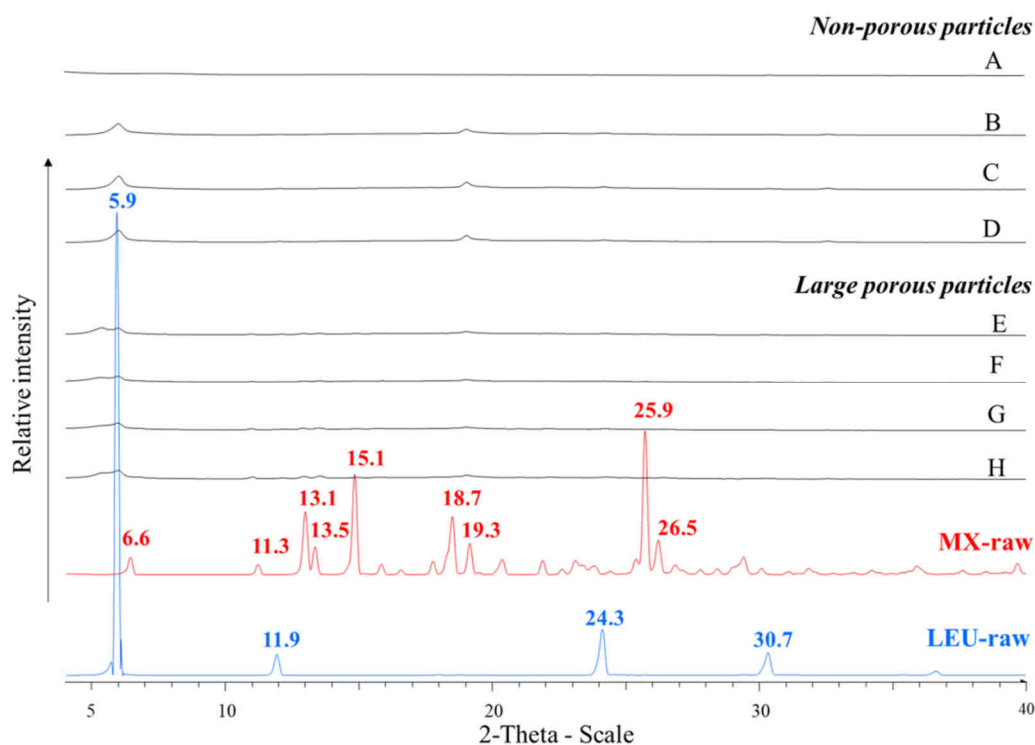
Fig. 4. XRPD spectra: The crystalline raw MX (MX-raw), and LEU (LEU-raw) are compared with the spray dried sample (A), non-porous particles (**B**: MX/LEU, **C**: MX/LEU/HA$^{0.3}$, **D**: MX/LEU/HA$^{0.15}$) and LPPs (**E**: MX/LEU/HA$^{0.3}$/AB$^{1.5}$, **F**: MX/LEU/HA$^{0.15}$/AB^2, **G**: MX/LEU/HA$^{0.15}$/AB$^{1.5}$, **H**: MX/LEU/HA$^{0.3}$/AB^2).

X-Ray powder diffraction was then used to characterize the crystalline state of MX after the spray drying process (**Fig. 4.**). The raw MX has characteristic peaks with the highest intensities at 6.6°, 11.4°, 13.1°, 13.5°, 15.1°, 18.7°, 19.3°, 25.9° and 26.4° 2-theta peaks indicating its crystalline structure (*Aytekin et al., 2018*). The fact that the characteristic peaks of crystalline MX are missing from the diffractogram of the spray dried sample (MX-SD) indicates that the raw material becomes amorphous when spray drying without excipients (**Fig. 4.** and **Supplementary material S1**). However, characteristic peaks of MX at 6.6°, 11.4°, 13°, 13.6° and 19.2° 2-theta appear in the formulations containing LEU (Supplementary Material S1), indicating a low level of crystallinity. We detected the same characteristic peaks of LEU that literature data reported (*Najafabadi et al., 2004; Li et al., 20016; Chvatal et al., 2017*). The characteristic peak 5.9° 2-theta of LEU could be observed on the spectra of the formulations but broader and with much lower intensity. These low intensity peaks demonstrate the low crystallinity of LEU after spray drying. The presence of HA has no effect on the diffractogram of the samples.

3.6 Aerodynamic properties

The aerodynamic properties (EF, FPF and MMAD) of powders were tested at 1st week and 10 weeks after the spray drying. No significant difference can be detected in the EF, FPF and

MMAD of the samples comparing the properties at 1st week and after 10 weeks storage (desiccator, 23±1 °C). The aerodynamic properties of the spray dried formulations remain unchanged.

An effect of excipients was observed for the non-porous formulations: those prepared with LEU have significantly higher EF than MX-SD. LEU increases the EF from ≤53.6% to ≥57.1%. LEU not just minimized the cohesion between particles, but also reduces the attachment to capsule wall during inhalation which resulted in higher EF values (*Aquino et al, 2012*; *Mangal et al., 2015*). However, contrary to other results showing that surface roughness lead to an increased FPF for LEU containing corrugated particles (*Chew et al, 2005*), we did not detect the FPF increasing effect of LEU. For the non-porous particles, the FPF remained in the 35-41% range independently of the excipients.

There are significant differences in the aerodynamic properties of LPPs and non-porous particles. LPPs result in higher EF and FPF than non-porous formulations (**Table III**). Briefly, the EF of the non-porous particles is not exceeding 62.1%, while LPPs EF are above 76.1% in all cases. The high EF of LPPs is related to the good flowability of particles and low adhesion to the capsule and device walls. It can be demonstrated, that the used AB concentrations have a relevant effect on the aerodynamic behaviour of LPPs. LPPs have significantly lower tap density (comparing to non-porous particles) which resulted improved lung deposition (FPF 54.5-65.8%). Bosquillon et al also established the same correlation between density and aerodynamics: the lower the tap density (0.04–0.25 g/cm^3), the higher the FPF (*Bosquillon et al, 2001*). LPP formulations prepared with 1.5 mg/mL AB concentrations have lower FPF (≤57.4%) than formulations containing 2.0 mg/mL AB (≥59.7%). The increased AB concentration (2.0 mg/mL) resulted in the highest FPF with 65.8% in case of MX/LEU/HA$^{0.15}$/AB^2 (measured at the 1st week). Despite the significant effect on the FPF, AB concentration has no significant effect on the EF of the LPPs. Comparing the LPP formulations, it can be concluded that HA content has no significant effect on the EF or FPF.

Table III. Comparison of the aerodynamic properties of the non-porous and large porous particles tested at 1st week and 10 weeks after spray drying simulating a 30 L/min inhalation flow rate. EF = emitted fraction, FPF = fine particle fraction. Data are represented as mean ±S.D., n=3.

Sample names	1st week		10th week	
	EF (%)	FPF (%)*	EF (%)	FPF (%)*
Non-porous particles				
MX-SD	53.6±10.5	38.6±4.7	50.4±6.7	37.9±4.8
MX/LEU	61.7±4.1	41.2±3.3	59.9±8.1	39.7±1.7
MX/LEU/HA$^{0.3}$	57.1±1.8	36.2±4.2	61.5±3.8	36.8±3.1
MX/LEU/HA$^{0.15}$	59.9±1.7	35.6±2.7	62.1±2.9	35.9±2.6
Large porous particles				
MX/LEU/HA$^{0.3}$/AB$^{1.5}$	79.5±4.2	54.5±2.1	79.4±2.3	55.9±2.3
MX/LEU/HA$^{0.15}$/AB$^{1.5}$	77.5±6.8	57.4±5.6	76.1±9.9	54.5±10.1
MX/LEU/HA$^{0.3}$/AB^{2}	79.5±5.5	59.7±4.0	85.4±3.2	60.5±1.6
MX/LEU/HA$^{0.15}$/AB^{2}	82.8±6.8	65.8±3.2	82.3±8.3	63.0±4.5

*FPF (<5 µm) was expressed with reference to the loaded dose.

The presented low density LPPs (≤0.19 g/cm^3) have better aerosolization properties (EF≥76.1% and FPF≥54.5%) and can reach the lower airways more easily than the smaller but denser non-porous particles (EF≤62.1% and FPF≤41.2%). Figure 5 demonstrates the relevance of the large geometric diameter (>5 µm) and low density (<0.25 g/cm^3) LPPs for lung delivery (**Fig. 5.**). LPPs and non-porous particles result in the same MMAD values (average 2.55 µm) with no significant differences. However, LPPs have larger geometric diameter (≤4.9 µm) than non-porous formulations. In case of non-porous formulations the increasing D[0.5] resulted in larger MMADs. In case of LPPs the MMAD is not increasing with the D[0.5]. Different effects were observed comparing the excipient concentrations just in case of LPPs. LPPs with 2.0 mg/mL AB concentration exhibit lower MMAD (2.41-2.32 µm) than those with 1.5 mg/mL (2.57-2.74 µm). The higher amount of porogen affected positively the flowability of the particles thus resulted in lower aerodynamic diameter. By contrast, there is no significant difference between the MMAD of 0.15 and 0.30 mg/mL HA concentrations.
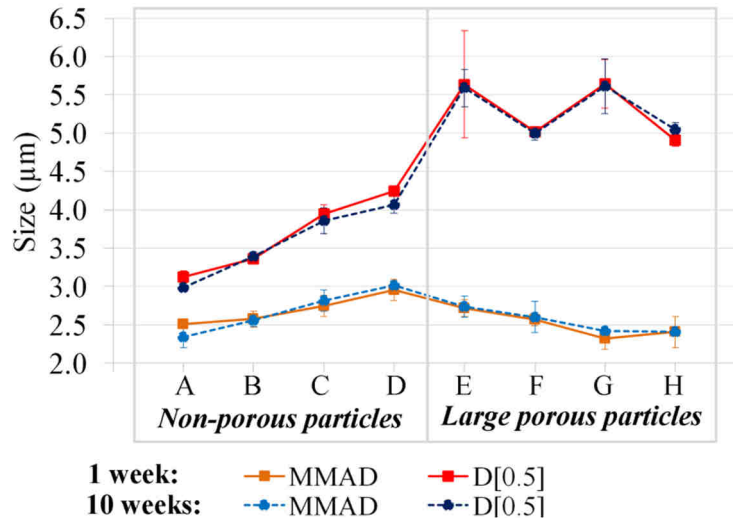
Fig. 5. Comparison of the aerodynamic and geometric diameter (MMAD = mass median aerodynamic diameter and D[0.5] = median geometric diameter) of the spray dried formulations. Data show the low density LPPs (E: $MX/LEU/HA^{0.3}/AB^{1.5}$, F: $MX/LEU/HA^{0.15}/AB^{1.5}$, G: $MX/LEU/HA^{0.3}/AB^2$ and H: $MX/LEU/HA^{0.15}/AB^2$) have the same or smaller MMAD than smaller but denser non-porous particles (A: MX-SD, B: MX/LEU, C: $MX/LEU/HA^{0.3}$ and D: $MX/LEU/HA^{0.15}$). Data are represented as mean ± S.D., n=3.

4 Conclusions

In the present study, two types of carrier-free DPIs were produced and compared: non-porous and LPP formulations of MX. We produced inhalable microparticles from MX aqueous solution with pH adjustment at pH 8±0.1, to facilitate the particle formulation process with in situ water soluble salt formation. Inhalable microparticles were produced with optimized spray drying conditions: 200 °C inlet temperature, 100% aspirator rate, 9 mL/min pump rate, and 414 L/h gas flow rate. LPPs with particle size larger than 4.9 µm and tap density lower than 0.19 g/cm^3 were obtained using 1.5 mg/mL MX, with 0.75 mg/mL LEU, 0.15 and 0.3 mg/mL HA; 1.5 and 2.0 mg/mL AB (samples $MX/LEU/HA^{0.3}/AB^{1.5}$, $MX/LEU/HA^{0.15}/AB^2$, $MX/LEU/HA^{0.15}/AB^{1.5}$ and $MX/LEU/HA^{0.3}/AB^2$). The aerosolization efficacies of the prepared LLPs were compared with the non-porous particles by testing the *in vitro* aerodynamical behaviour (with Andersen Cascade Impactor). The study was carried out using 30 L/min to simulate the low inhalation flow rate characteristic of lung inflammation diseases. LPPs show EF above ≥77.5% and FPF above ≥54.5%, both exceeding the non-porous particles values. The aerodynamical properties remain unchanged after 10 weeks of storage for all formulations. The concentration of AB, a porogen agent used in the primary solutions is a critical parameter of the LPP formulation. The best considered LPPs (with the highest spray drying yield ≥62% and FPF reaching 65.8%) were the ones containing 2 mg/mL AB as porogen beside the appropriate concentration of LEU and HA (samples $MX/LEU/HA^{0.3}/AB^2$ and $MX/LEU/HA^{0.15}/AB^2$). The presented aerodynamic properties have no significant difference measured after 1 and 10 weeks of storage. Thanks to the good aerosolization properties, the presented LPPs containing MX may offer an effective local treatment for lung inflammation diseases and should be tested in vivo in a near future.

5 Acknowledgements

References

Aquino, R.P., Prota, L., Auriemma, G., Santoro, A., Mencherini, T., Colombo, G., Russo, P. 2017. Dry powder inhalers of gentamicin and leucine: formulation parameters, aerosol performance and in vitro toxicity on CuFi1 cells. Int. J. Pharm. 426, 100– 107. https://doi:10.1016/j.ijpharm.2012.01.026

Arafa, M.M.H., Abdel-Wahab, M.H., El-Shafeey, M.F., Badary, O.A., Hamada, F.M.A. 2007. Anti-fibrotic effect of meloxicam in a murine lung fibrosis model. Eur. J. Pharmacol. 564, 181– 189. https://doi.org/10.1016/j.ejphar.2007.02.065

Aytekin, Y.S., Köktürk, M., Zaczek, M., Korter, T.M., Heilweil, E.J., Esenturk, O. 2018. Optical properties of Meloxicam in the far-infrared spectral region. Chem. Phys. 512, 36–43. https://doi.org/10.1016/j.chemphys.2018.04.022

Bio-Rad Laboratories, Inc. SpectraBase; SpectraBase Compound ID=1uNoyEsAnyk SpectraBase Spectrum ID=DBmpr8dVTkQ http://spectrabase.com/spectrum/DBmpr8dVTkQ (accessed Nov 05, 2018).

Bosquillon, C., Lombry, C., Preat, V., Vanbever, R. 2001. Influence of formulation excipients and physical characteristics of inhalation dry powders on their aerosolization performance. J. Control. Release 70, 329–339. https://doi.org/10.1016/S0168-3659(00)00362-X

Chvatal, A., Farkas, Á., Balásházy, I., Szabó-Révész, P., Ambrus, R. 2017. Structural and aerodynamic evaluation of microcomposites containing meloxicam potassium. Int. J. Pharm. 520, 70–78. https://doi.org/10.1016/j.ijpharm.2017.01.070

Cruz, L., Fattal, E., Tasso, L., Freitas, G.C., Carregaro, A.B., Guterres, S.S., Pahlomann, A.R., Tsapis, N. 2011. Formulation and in vivo evaluation of sodium alendronate spray-dried microparticles intended for lung delivery. J. Control. Release 152, 370–375. https://doi.org/10.1016/j.jconrel.2011.02.030

Chew, N., Tang, P., Chan, H.K., Raper, J.A. 2005. How Much Particle Surface Corrugation Is Sufficient to Improve Aerosol Performance of Powders? Pharm Res. 22: 148. https://doi.org/10.1007/s11095-004-9020-4

Colombo, P., Traini, D., Buttini, F. 2012. Inhalation drug delivery: techniques and products. Chapter6. John Wiley & Sons (ISBN 978-1-18-35412-4).

European Pharmacopoeia Online 9.6, Chapter 2.9.18. Preparations for inhalation: aerodynamic assessment of fine particles. (Last accessed on 28 November 2018).

European Pharmacopoeia Online 9.6, Chapter 2.9.34. Bulk density and tapped density of powders. (Last accessed on 28 November 2018).

Gervelas, C., Serandour, A.L., Geiger, S., Grillon, G., Fritsch, P., Taulelle, C., Le Gall, B., Benech, H., Deverre, J.R., Fattal, E., Tsapis, N. 2007. Direct lung delivery of a dry powder formulation of DTPA with improved aerosolization properties: Effect on lung and systemic decorporation of plutonium. J. Control. Release. 118, 78–86. https://doi.org/10.1016/j.jconrel.2006.11.027

Healy, A.M., Amaro, M.I., Paluch, K.J., Tajber, L. 2014. Dry powders for oral inhalation free of lactose carrier particles. Adv. Drug Deliver. Rev. 75, 33–52. https://doi.org/10.1016/j.addr.2014.04.005

Hoppentocht, M., Hagedoorn, P., Frijlink, H.W., de Boer, A.H. 2014. Technological and practical challenges of dry powder inhalers and formulations. Adv. Drug Deliver. Rev. 75, 18–31. https://doi.org/10.1016/j.addr.2014.04.004

Horváth, T., Ambrus, R., Völgyi, G., Budai-Szűcs, M., Márki, Á., Sipos, P., Bartos, Cs., Seres, A.B., Sztojkov-Ivanov, A., Takács-Novák, K., Csányi, E., Gáspár, R., Szabó-Révész, P. 2016. Effect of solubility enhancement on nasal absorption of meloxicam. Eur. J. Pharm. Sci. 95, 96–102. https://doi.org/10.1016/j.ejps.2016.05.031

Lechuga-Ballesteros, D., Charan, C., Stults, C.L.M., Stevenson, C.L., Miller, D.P., Vehring, R., Tep, V., M.C. 2008. Trileucine Improves Aerosol Performance and Stability of Spray-Dried Powders for Inhalation. J. Pharm. Sci. 97, 287–302. https://doi.org/10.1002/jps.21078

Li, Q., Rudolph V., Weigl B., Earl A. 2004. Interparticle van der Waals force in powder flowability and compactibility. Int. J. Pharm. 280, 77–93. https://doi.org/10.1016/j.ijpharm.2004.05.001

Li, L., Sun, S., Parumasivam, T., Denman, J.A., Gengenbach, T., Tang, P., Mao, S., Chan, H.K. 2016. L-Leucine as an excipient against moisture on in vitro aerosolization performances of highly hygroscopic spray-dried powders. Eur. J. Pharm. Biopharm. 102, 132–141. https://doi.org/10.1016/j.ejpb.2016.02.010

Li, Y., Han, M., Liu, T., Cun, D., Fang, L., Yang, M. 2017. Inhaled hyaluronic acid microparticles extended pulmonary retention and suppressed systemic exposure of a short-acting bronchodilator. Carbohydrate Polymers. 172, 197-204. https://doi.org/10.1016/j.carbpol.2017.05.020

Mangal, S., Meiser, F., Tan, G., Gengenbach, T., Denman, J., Rowles, M.R., Larson, I., Morton, D.A.V. 2015. Relationship between surface concentration of L-leucine and bulk powder properties in spray dried formulations. Eur. J. Pharm. Biopharm. 94, 160–169. https://doi.org/10.1016/j.ejpb.2015.04.035

Martinelli, F., Balducci, A.G., Kumar, A, Sonvico, F., Forbes, B., Bettini, R., Buttini, F. 2017. Engineered sodium hyaluronate respirable dry powders for pulmonary drug delivery Int. J. Pharm. 517, 286–295. https://doi.org/10.1016/j.ijpharm.2016.12.002

Mezei, T., Mesterházy, N., Bakó, T., Porcs-Makkay, M., Simig, G., Volk, B. 2009. *Manufacture of high-purity meloxicam via its novel potassium salt monohydrate* Org. Process Res. Dev. 13, 567–572. https://pubs.acs.org/doi/abs/10.1021/op900031h

Najafabadi A.R., 2004. *The effect on vehicle on physical properties and aerolization behaviour of disodium cromoglycate microparticles spray dried alone or with L-leucine.* Int. J. Pharm., 285, 97-108. https://doi.org/10.1016/j.ijpharm.2004.07.027

N'Guessan, A., Fattal, E., Chapron, D., Gueutin, C., Koffi. A., Tsapis, N. 2018. *Dexamethasone palmitate large porous particles: A controlled release formulation for lung delivery of corticosteroids.* Eur. J. Pharm. Sci. 113, 185–192. http://dx.doi.org/10.1016/j.ejps.2017.09.013

Lorraine M. Nolan, Lidia Tajber, Bernard F. McDonald, Ahmad S. Barham, Owen I. Corrigan, Anne Marie Healy. 2009. *Excipient-free nanoporous microparticles of budesonide for pulmonary delivery.* Eur. J. Pharm. Sci. 37, 593–602. https://doi:10.1016/j.ejps.2009.05.007

Ógáin, O.N., Li, J., Tajber, L., Corrigan, O.I., Healy, A.M. 2011. *Particle engineering of materials for oral inhalation by dry powder inhalers. I—Particles of sugar excipients (trehalose and raffinose) for protein delivery.* Int. J. Pharm. 405, 23–35. https://doi.org/10.1016/j.ijpharm.2010.11.039

Ogienko, A.G., Bogdanova, E.G., Trofimov, N.A., Myzd, S.A., Ogienko, A.A., Kolesov, B.A, Yunoshev, A.S., Zubikov, N.V., Manakov, A.Yu., Boldyrev, V.V., Boldyrev, E.V. 2017. *Large porous particles for respiratory drug delivery. Glycine-based formulations.* Eur. J. Pharm. Sci. 110, 148–156. https://doi.org/10.1016/j.ejps.2017.05.007

Pham, D.-D., Fattal, E., Ghermani, N., Guiblin, N., Tsapis, N. 2013. *Formulation of pyrazinamide-loaded large porous particles for the pulmonary route: Avoiding crystal growth using excipients.* Int. J. Pharm. 454, 668– 677. https://doi.org/10.1016/j.ijpharm.2013.04.016

Pham, D.-D., Grégoire, N., Couet, W., Gueutin, C., Fattal, E., Tsapis, T. 2015. *Pulmonary delivery of pyrazinamide-loaded large porous particles.* Eur. J. Pharm. Biopharm. 94, 241–250. https://doi.org/10.1016/j.ejpb.2015.05.021

Pomázi, A., Ambrus R., Sipos P., Szabó-Révész P. 2011. *Analysis of co-spray-dried meloxicam-mannitol systems containing crystalline microcomposites.* Journal of Pharmaceutical and Biomedical Analysis. 56, 183-190. https://doi.org/10.1016/j.jpba.2011.05.008

Pomázi, A., Ambrus R., Szabó-Révész P. 2014. *Physicochemical stability and aerosolization performance of mannitol-based microcomposites.* J. Drug Del. Sci. Tech. 24, 397-403. https://doi.org/10.1016/S1773-2247(14)50080-9

Pomázi, A., Buttini, F., Ambrus, R., Colombo, C., Szabó-Révész, P. 2013. *Effect of polymers for aerolization properties of mannitol-based microcomposites containing meloxicam.* European Polymer Journal. 49, 2518-2527. https://doi.org/10.1016/j.eurpolymj.2013.03.017

Raula, J., Thielmann, F., Naderi, M., Lehto, V.P., Kauppinen, E.I. 2010. *Investigations on particle surface characteristics vs. dispersion behaviour of l-leucine coated carrier-free inhalable powders.* Int. J. Pharm. 385, 79–85. https://doi.org/10.1016/j.ijpharm.2009.10.036

Simon, A., Amaro, M.I., Cabral, L.M., Healy, A.M. 2016. Development of a novel dry powder inhalation formulation for the delivery of rivastigmine hydrogen tartrate. Int. J. Pharm. 501, 124–138. https://doi.org/10.1016/j.ijpharm.2016.01.066

Szabó-Révész P. 2018. Modifying the physicochemical properties of NSAIDs for nasal and pulmonary administration, Drug Discov Today: Technol. https://doi.org/10.1016/j.ddtec.2018.03.002

Tsapis, N. 2014. Spray-drying from fundamentals to pulmonary administration of therapeutic molecules. Rev. Farmacol. Chile. 7(2), 33-40.

Tsubouchi, Y., and Al, E. 2000. Meloxicam inhibits the growth of non-small cell lung cancer. Anticancer Res. 20, 2867–2872.

Vehring, R., 2008. Pharmaceutical particle engineering via spray drying. Pharm. Res. 25, 999–1022. https://doi.org/10.1007/s11095-007-9475-1

Watts, A.B., Wang, Y.B., Johnston, K.P., Williams III, R.O. 2013. Respirable Low-Density Microparticles Formed In Situ from Aerosolized Brittle Matrices. Pharm. Res. 30, 813–825. https://doi.org/10.1007/s11095-012-0922-2
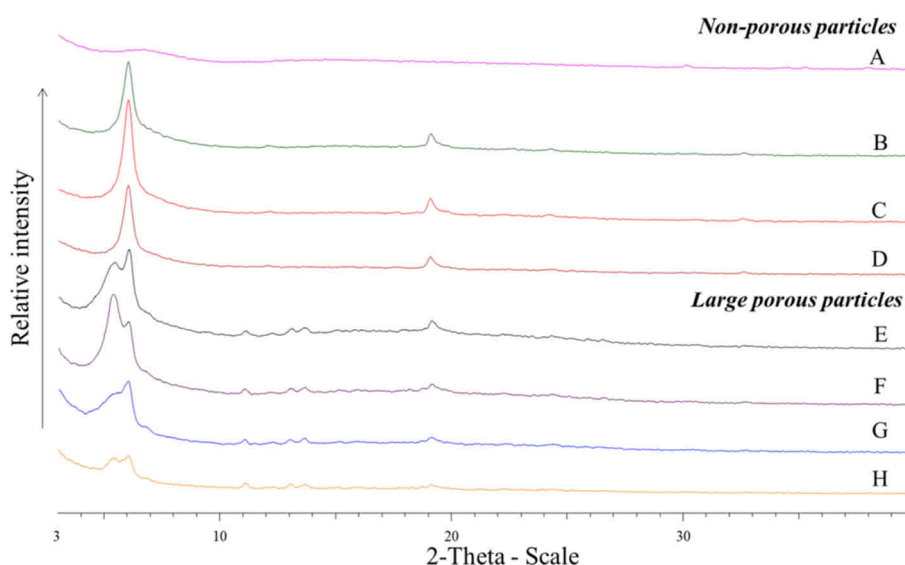
Supplementary Material

Figure S1: Zoom on the diffractograms of the spray dried samples (A), non-porous particles (**B**: MX/LEU, **C**: MX/LEU/HA$^{0.3}$, **D**: MX/LEU/HA$^{0.15}$) and LPPs (**E**: MX/LEU/HA$^{0.3}$/AB$^{1.5}$, **F**: MX/LEU/HA$^{0.15}$/AB^2, **G**: MX/LEU/HA$^{0.15}$/AB$^{1.5}$, **H**: MX/LEU/HA$^{0.3}$/AB^2).